



## Microstructure and mechanical properties of NiCoCrAlY laser cladding coating after high-current pulsed electron beam irradiation

Bowen Chen, Yuxin Li, Jinhao Nie, Chen Wei, Lihua Dang & Qingjun Ma

**To cite this article:** Bowen Chen, Yuxin Li, Jinhao Nie, Chen Wei, Lihua Dang & Qingjun Ma (2023) Microstructure and mechanical properties of NiCoCrAlY laser cladding coating after high-current pulsed electron beam irradiation, *Philosophical Magazine Letters*, 103:1, 2191223, DOI: [10.1080/09500839.2023.2191223](https://doi.org/10.1080/09500839.2023.2191223)

**To link to this article:** <https://doi.org/10.1080/09500839.2023.2191223>



© 2023 The Author(s). Published by Informa UK Limited, trading as Taylor & Francis Group



Published online: 20 Mar 2023.



Submit your article to this journal [↗](#)



Article views: 2691



View related articles [↗](#)



View Crossmark data [↗](#)

# Microstructure and mechanical properties of NiCoCrAlY laser cladding coating after high-current pulsed electron beam irradiation

Bowen Chen<sup>a,b</sup>, Yuxin Li<sup>c</sup>, Jinhao Nie<sup>d</sup>, Chen Wei<sup>a,b</sup>, Lihua Dang<sup>a,b</sup> and Qingjun Ma<sup>a,b</sup>

<sup>a</sup>Tianjin Special Equipment Inspection Institute, Tianjin, People's Republic of China; <sup>b</sup>National Supervision and Inspection Center for Special Equipment Welding Consumables Quality, Tianjin, People's Republic of China; <sup>c</sup>School of Materials Science and Engineering, North University of China, Taiyuan, People's Republic of China; <sup>d</sup>School of Material Science and Engineering, Harbin Institute of Technology, Harbin, People's Republic of China

## ABSTRACT

Surface modification of laser cladding coating NiCoCrAlY was carried out by high-current pulsed electron beam irradiation. The microstructure of the NiCoCrAlY coating after irradiation was studied by XRD and SEM. The results showed that the NiCoCrAlY cladding layer displays slip and a nanocrystalline structure following high-current pulsed electron beam irradiation. The high-density slip structure affects the residual stress on the surface of the melted coating, resulting in a change of the phase structure. The mechanical properties of the NiCoCrAlY coating were studied using a Vickers micro-hardness tester and a straight-line-reciprocating dry sliding wear tester. The results showed the average microhardness of the melted coating increased by 9%, and the average wear coefficient decreased by 33.7% after five electron beam irradiations.

## ARTICLE HISTORY



Received 22 August 2022  
Accepted 10 March 2023

## KEYWORDS

Laser cladding; high-current pulsed electron beam irradiation; microhardness; wear

## 1. Introduction

As a representative advanced manufacturing technology, surface treatment technology has been widely studied and developed in recent years [1, 2]. Laser cladding technology, is also known as laser metal deposition technology, is a new type of surface treatment [3, 4]. In laser cladding, the coupling between the laser and substrate, laser and powder, and substrate and powder is carefully designed and controlled. Although optimal process parameters can be determined experimentally, residual stress [5] or crystal precipitation [6] can occur in the cladding coating owing to complex interactions between laser

**CONTACT** Yuxin Li  lyx\_nuc@163.com  School of Materials Science and Engineering, North University of China, Taiyuan 030051, People's Republic of China

© 2023 The Author(s). Published by Informa UK Limited, trading as Taylor & Francis Group  
This is an Open Access article distributed under the terms of the Creative Commons Attribution License (<http://creativecommons.org/licenses/by/4.0/>), which permits unrestricted use, distribution, and reproduction in any medium, provided the original work is properly cited. The terms on which this article has been published allow the posting of the Accepted Manuscript in a repository by the author(s) or with their consent.

energy, powder, and substrate, thus causing surface cracks in the cladding coating, which affects its mechanical properties [7].

As an advanced surface treatment using energetic beams [1, 8], high-current pulsed electron beam (HCPEB) technology allows for greater control of the injected energy. Using this technology, a high-temperature gradient can be formed in the surface layer of the material to a depth of tens of microns, resulting in a rapid and strong deformation of the surface of the material. Many researchers use HCPEB technology to modify metal surfaces to improve their mechanical or corrosion resistance. Gao et al. [9] improved the microhardness of TC4 alloy by regulating the energy density of the HCPEB. Wu et al. [10] suggested that a reasonable number of HCPEB irradiations could improve the corrosion resistance of AZ91 magnesium alloy. Gao et al. [11] formed a bilayer hyperfine crystal structure in the surface layer of Al-20Si-5Mg using HCPEB irradiation, which improved its mechanical properties.

In this study, a NiCoCrAlY coating prepared by laser cladding technology was irradiated by a HCPEB. The evolution of the phase structure and microstructure of the NiCoCrAlY cladding layer was studied, and its hardness, friction, and wear properties after irradiation evaluated.

## 2. Experimental details

NiCoCrAlY metal powder purchased from the Hunan Metallurgical Institute was dried in a vacuum oven at 120°C for 24 h before the laser cladding treatment. A coating layer approximately 1.5 mm thick was then prepared on the surface of a 20 × 20 × 10 mm 304 stainless steel sample using a German Laserline Gmbn fiber-coupled semiconductor laser. The chemical composition of the NiCoCrAlY powder is shown in Table 1. The laser cladding process parameters were a laser power of 1600 W, a scanning speed of 8 mm/s, and an overlap size of 50%. The HCPEB equipment used was a Nadezhda-2 system. The main experimental parameters were as follows: electron beam energy 27 keV, energy density 4 J/cm<sup>2</sup>, pulse width 1.5 μm, pulse interval 10 s, and number of pulses 5 and 15. Mechanical experiments were conducted to measure the microhardness, friction, and wear properties before and after HCPEB irradiation. A micro-Vickers hardness test was carried out on a JMHSV-1000AT microhardness tester with a load of 200 g and a holding time of 5 s. The friction and wear properties at room temperature (298.15 K) were measured using an HSR-2M high-speed reciprocating friction tester. The experimental load was 10 N and the single experiment time was 30 min. The

**Table 1.** Chemical composition of NiCoCrAlY powder (wt.%).

Element	Ni	Co	Cr	Al	Y	O
Content	Bal.	22.92	17.08	12.81	0.49	0.08

friction pair material was a  $\text{Si}_3\text{N}_4$  ceramic ball with a diameter of 4 mm. The phase composition of the NiCoCrAlY laser cladding layer before and after HCPEB irradiation was analysed by X-ray diffraction (XRD) using a Cu  $\text{K}\alpha$  X-ray diffractometer. The morphologies of the worn surfaces of the coatings were investigated by scanning electron microscopy.

### 3. Results and discussion

Figure 1 shows the phase composition changes of the NiCoCrAlY coating before and after HCPEB irradiation. It can be seen from the figure that the HCPEB irradiation did not affect the phase composition. The NiCoCrAlY coating before and after irradiation was composed of  $\gamma/\gamma'$  and  $\beta$ -NiAl phases with a face-centered cubic structure. However, with increasing irradiation time, the diffraction peaks moved to high angles and gradually broadened. According to the Bragg equation (formula 1) and the Scherrer formula (formula 2)

$$d = n\lambda/2 \sin \theta \quad (1)$$

$$D_{\text{hkl}} = k\lambda/\beta\cos\theta_{\text{hkl}} \quad (2)$$

it can be seen that the reason for this is refinement of the grains of the NiCo-CrAlY fusion layer. When X-rays are incident on the small crystals, the diffraction line becomes dispersed and widens. Combined with the work of Zou et al. [12] and Chai et al. [13], it can be seen that thermal stress and thermal fields formed on the surface of the metal fusion blanket owing to HCPEB irradiation, resulting in rapid heating and cooling. The accompanying stress resulted in a

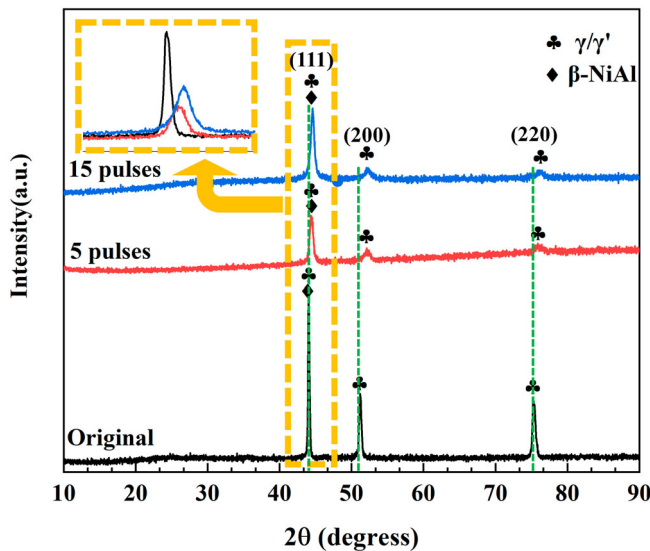
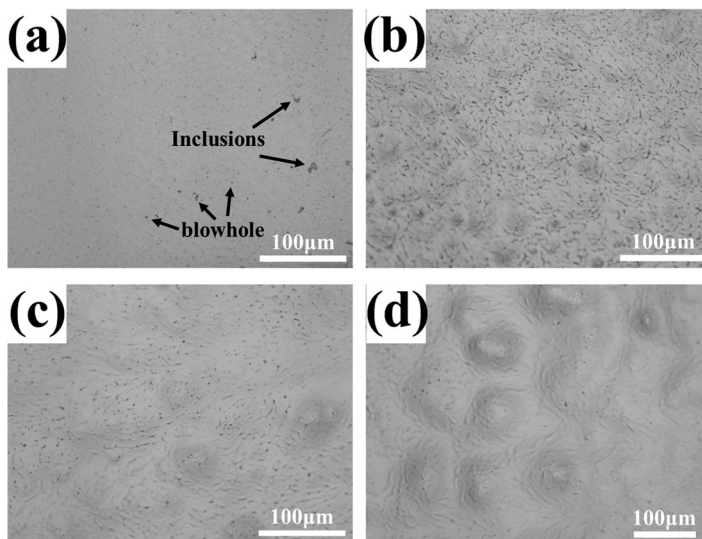


Figure 1. XRD patterns of NiCoCrAlY cladding layers subjected to HCPEB.

solidification texture on the surface of the fusion blanket and macroscopically affected the blanket's mechanical properties.

Figure 2a–d shows the morphologies of the NiCoCrAlY coating surface before and after HCPEB. Figure 2a shows a micrograph of the original NiCoCrAlY fused layer after polishing. It can be seen that the polished fused layer contained many pores and inclusions. Figure 2b–c shows the surface morphology after 5 and 15 pulses of HCPEB irradiation, respectively. After 5 pulses of irradiation, many second-phase elements had escaped from the melted layer surface. The high-temperature gradient generated by the HCPEB led to the immediate evaporation of defects and inclusions from the melted layer surface. The evaporated impurities then condensed on the surface of the irradiated layer on account of rapid cooling. During the evaporation–recondensation process under 5 pulses of irradiation, the evaporation mode dominated [14], resulting in a morphology characteristics of the melted layer shown in Figure 2b. Upon increasing the number of pulses to 15 (Figure 2c), the multiple rapid cooling–solidification cycles further purified the melted layer surface. The multiple pulses increased the storage entropy of the melted layer surface and the subsurface, which induced a stronger current and further evaporation. In this case, most of the impurities in the melted layer and the redeposited layer were removed, such that the NiCoCrAlY irradiated layer after 15 pulses was cleaner.

It is worth noting that Figure 2b–c shows different numbers and sizes of melted peak and valley structures, with the number of crater structures decreasing with increasing pulse time. According to references [15–17], these

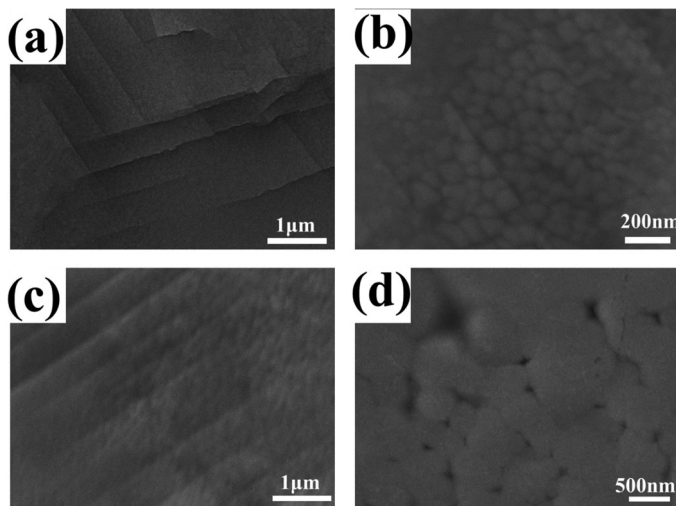


**Figure 2.** SEM images of (a) initial NiCoCrAlY alloy surface and (b–c) NiCoCrAlY alloy surfaces after (b) 5 and (c) 15 pulses. (d) Typical crater map after irradiation. (e–f) Typical grains and slip lines after 5 pulses.

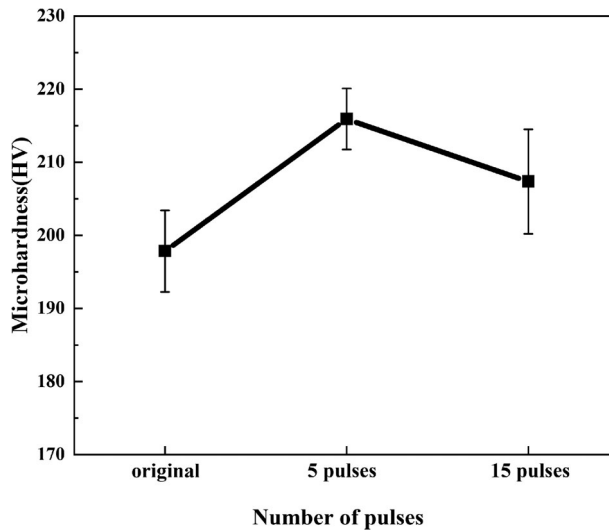
characteristics arise from a melt-blown mechanism. That is, under the influence of pulse irradiation, the coating begins to melt from the subsurface, resulting in the formation of small droplets at the grain boundaries. With further irradiation, and thus increasing temperature, the droplets continue to grow. Some erupt under the action of interfacial stress, whereas some continue to grow until the irradiation is completed. At this time, the small droplets make contract owing to the cooling effect, forming a funnel-shaped crater morphology. The number and morphology of the craters are related to the number of irradiation cycles. In general, the more the number of pulse irradiation times, the higher the number of small droplets are sprayed and purified, and the number of droplets without spraying grow with heating time.

Figure 3a–b shows typical SEM images of the melted layer after five HCPEB cycles. There are different angles between the sliding lines and numerous nanocrystalline structures form around the sliding lines [14, 18]. The main reason for these results is boiling in the evaporation mode. Many small bubbles dissolve, evaporate, and are deposited from the liquid melt, a process that is repeated until a more stable condensation nucleus is formed at the end of irradiation. Many nanoscale deposited particles are formed during the ultrafast cooling process. After 15 irradiation cycles, the grain size increased significantly, as shown in Figure 3c–d. This is because the cooling of the cladding layer after HCPEB irradiation occurs mainly through heat conduction of the matrix. With an increase in the number of irradiation cycles, the heat conduction rate of the matrix decreases, resulting in a decrease in the supercooling degree of the molten layer front and grain growth.

Figure 4 shows the microhardness of the NiCoCrAlY fusion layer before and after HCPEB irradiation. It can be seen that the surface microhardness of the



**Figure 3.** SEM images of typical grains and slip lines after (a–b) 5 and (c–d) 15 pulses.



**Figure 4.** Microhardness of NiCoCrAlY cladding layer after HCPEB irradiation.

coating after irradiation was higher than that of the original coating. However, the hardness is not linearly correlated with the number of pulsed electron beam irradiations. The average microhardness of the cladding layer surface after 5 pulse treatments is the largest, reaching 216 HV<sub>0.2</sub>.

The reason for the increase in microhardness of the NiCoCrAlY coating layer after HCPEB irradiation is that irradiation causes rapid local heating and melting of the sample surface in a nearly adiabatic manner, followed by rapid solidification caused by the self-excited cooling of the matrix itself. During the cooling and solidification process, the irradiation layer changes from a liquid to a solid phase to form nanocrystals; that is, fine-grain strengthening occurs during pulse irradiation, which affects the microhardness of the coating surface. A large number of nanocrystallites appear in the coating after 5 pulse irradiations (see Figure 3). Thus, the microhardness of the coating after 5 pulse irradiations is the highest. The difference in hardness behaviour between coatings is closely related to the microstructure and phase composition of the coatings [19]. In an MCrAlY superalloy, the microhardness of the  $\beta$  phase is higher than that of the  $\gamma$  phase. After HCPEB irradiation, the elements on the coating surface are further homogenised and Al is more likely to combine with Ni to form an aluminum-rich  $\beta$ -NiAl phase. Therefore, the microhardness of the current coating was further strengthened after irradiation [20].

Figure 5a–b shows the variations of the wear coefficient and amount of wear of the NiCoCrAlY coating before and after HCPEB irradiation. It can be seen from Figure 5a that the friction coefficient of the NiCoCrAlY coating tended to stabilise 2 min after the friction and wear experiment, indicating that the coating had good moulding quality and uniform surface and internal components. The friction, the wear coefficient and the amount of wear of the



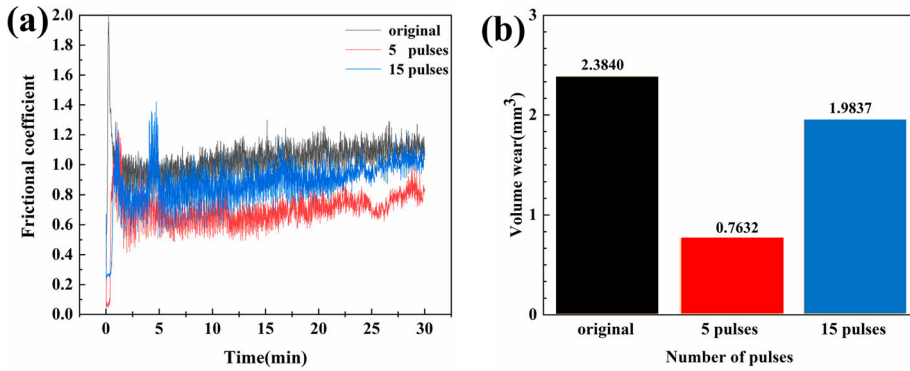


**Figure 5.** (a) Wear coefficient and (b) wear amount before and after HCPEB irradiation.

coating surface irradiated by HCPEB were all over than those of the original coating, indicating that HCPEB irradiation improved the friction and wear properties of the coating. The average friction coefficient of the original fusion layer was 1.04, whereas it was 0.70 after 5 pulses of irradiation and 0.89 after 15 pulses. Compared with the original coating, the wear volume decreased by 66.9% after 5 pulses of irradiation, indicating that the wear resistance of the NiCoCrAlY coating was relatively good after 5 pulses of irradiation.

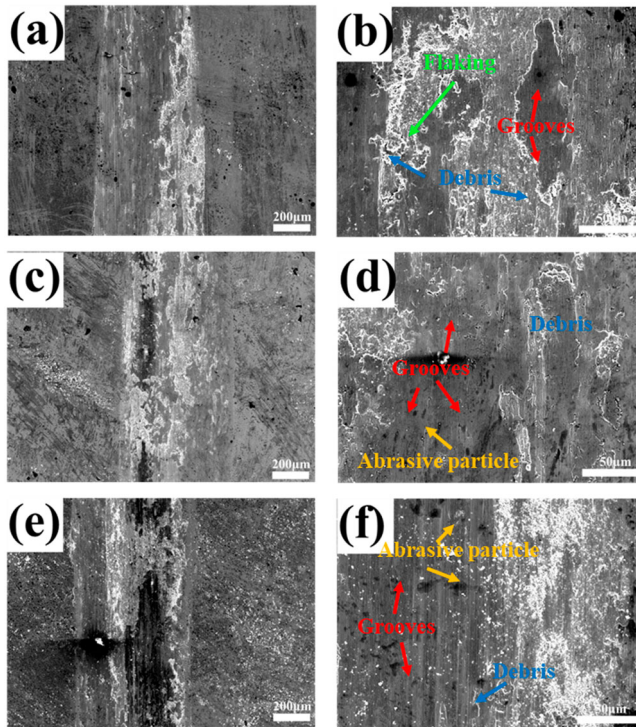


**Figure 6.** The worn surface morphologies of the substrate and HCPEB surface: (a–b) original, (c–d) after 5 pulses, and (e–f) after 15 pulses.



Figure 6 shows a SEM image of the NiCoCrAlY coating after HCPEB irradiation showing the result of friction and wear testing. It can be seen in the figure that the coating after friction and wear testing consists mainly of furrows and debris. It is worth noting that the surface wear morphology of the coating irradiated by HCPEB after 5 pulses is mainly furrow-like because the surface wear resistance of the coating after 5 pulses of irradiation was good and thus not easy to deform. The main wear mechanism of the coating is abrasive wear [21]. Compared to the coating after 5 pulses, the original NiCoCrAlY coating had more debris on the worn surface, which led to a certain amount of spalling on the worn surface. The main reason for the difference in the wear morphology between the two coatings is that there were pores on the surface of the original coating owing to the laser-cladding coating. The fracture of pores leads to the change of the surface stress of the coating, which assists the coating surface to fall off.

At room temperature, the main wear mechanism of the NiCoCrAlY coating was a combination of abrasive wear and adhesive wear. At the edge of the wear scar, plastic deformation occurred on the coating surface under the action of friction. At the same time, high-speed reciprocating wear generated heat on the worn surface by friction, resulting in a slight oxidation reaction on the coating surface. The surface oxidation of the NiCoCrAlY coating generated protective oxides such as  $\text{Al}_2\text{O}_3$  and  $\text{Cr}_2\text{O}_3$ . The adhesion between the oxides and the NiCoCrAlY coating was relatively high, but the formation and removal of oxides were caused by mechanical action during friction and wear. Therefore, layering of the coating occurs in some regions as can be seen in Figure 6. It is worth noting that, compared with the melted coating after 5 pulses of irradiation, there was more delamination in the melted coating after 15 pulses. There are two possible reasons for this. First, owing to multiple irradiations, the surface remelted many times. Compared with the 5 pulses, the grains of the coating after 15 pulses of irradiation grew into coarse grains that were prone to brittle cracking during the friction and wear process, resulting in significant spalling and a large amount of debris. The second reason is that multiple re-melting led to a more uniform formation of elements on the coating surface and, thereby, various oxides were formed earlier in the wear process. The high viscosity of oxides led to delamination of the coating during the wear process.

#### 4. Conclusions

- (1) A residual stress in a NiCoCrAlY fusion layer was induced by high-current pulsed electron beam irradiation. The diffraction peak of the fusion layer shifted to a higher angle after irradiation.

- (2) Slip lines and a nanocrystalline structure appeared on the surface of the fusion layer as a consequence of the high-current pulsed electron beam irradiation.
- (3) The mechanical properties of the fusion layer after irradiation were greatly improved. The average microhardness of the melted coating increased by 9%, and the average wear coefficient decreased by 33.7% after 5 irradiations.
- (4) Wear features of the NiCoCrAlY coating occurred during high-current pulsed electron beam irradiation owing to a combination of abrasive and adhesive wear.

### Disclosure statement

No potential conflict of interest was reported by the author(s).

### Funding

We gratefully acknowledge the support of the National Natural Science Foundation of China [U1810112] and a Research Project Supported by Shanxi Scholarship Council of China [2021-126].

### Notes on contributors

**Bowen Chen**, Master, the main research direction is laser surface modification technology.

**Yuxin Li**, Doctor, Professor, the main research direction is laser additive manufacturing technology.

**Jinhao Nie**, Doctor, the main research direction is laser surface repair technology.

**Chen Wei**, Doctor, Senior engineer, the main research direction is solid phase welding technology.

**Lihua Dang**, Senior engineer, the main research direction is metal coating corrosion.

**Qingjun Ma**, Master, the main research direction is the physical and chemical inspection technology of welding materials.

### References

- [1] Y. Qin, J.X. Zou, C. Dong, X.G. Wang, A.M. Wu, Y. Liu, S.Z. Hao, and Q.F. Guan, *Temperature-stress fields and related phenomena induced by a high current pulsed electron beam*. Nucl. Instrum. Methods Phys. Res. B-Beam Interact. Mater. At. 225 (2004), pp. 544–554.
- [2] W. Yuan, D.D. Xia, S.L. Wu, Y.F. Zheng, Z.P. Guan, and J.V. Rau, *A review on current research status of the surface modification of Zn-based biodegradable metals*. Bioact. Mater. 7 (2022), pp. 192–216.
- [3] R.M. Mahamood, *Laser Metal Deposition Process of Metals, Alloys, and Composite Materials*, Springer, Cham, 2018, p.197–210.

- [4] A.G. Demir and B. Previtali, *Laser metal deposition employing scanning optics*. Lasers Eng. 40 (2018), pp. 297–316.
- [5] S.L. Wang, Z.Y. Zhang, Y.B. Gong, and G.M. Nie, *Microstructures and corrosion resistance of Fe-based amorphous/nanocrystalline coating fabricated by laser cladding*. J. Alloys Compd. 728 (2017), pp. 1116–1123.
- [6] M.F. de Carvalho, R. Riva, J.B. Fogagnolo, C.S. Kiminami, and C.R.M. Afonso, *Metallic glass formation upon rapid solidification of Fe<sub>60</sub>Cr<sub>8</sub>Nb<sub>8</sub>B<sub>24</sub> (at%) alloy through LASER cladding and remelting*. Mater. Res. Ibero Am. J. Mater. 20 (2017), pp. 580–587.
- [7] J.E. Garcia-Herrera, J. Henao, D.G. Espinosa-Arbelaez, J.M. Gonzalez-Carmona, C. Felix-Martinez, R. Santos-Fernandez, J. Corona-Castuera, C.A. Poblano-Salas, and J.M. Alvarado-Orozco, *Laser cladding deposition of a Fe-based metallic glass on 304 stainless steel substrates*. J. Therm. Spray Technol. 31 (2022), pp. 968–979.
- [8] Q.F. Guan, H. Zou, G.T. Zou, A.M. Wu, S.Z. Hao, J.X. Zou, Y. Qin, C. Dong, and Q.Y. Zhang, *Surface nanostructure and amorphous state of a low carbon steel induced by high-current pulsed electron beam*. Surf. Coat. Technol. 196 (2005), pp. 145–149.
- [9] Y.K. Gao, *Surface modification of TC4 titanium alloy by high current pulsed electron beam (HCPEB) with different pulsed energy densities*. J. Alloys Compd. 572 (2013), pp. 180–185.
- [10] P.P. Wu, K.K. Deng, K.B. Nie, and Z.Z. Zhang, *Corrosion resistance of AZ91 Mg alloy modified by high-current pulsed electron beam*. Acta Metall. Sin.-Engl. Lett. 32 (2019), pp. 218–226.
- [11] B. Gao, K. Li, and P.F. Xing, *Formation of a double-layer ultrafine crystal structure for high-current pulsed electron beam-treated Al-20Si-5Mg alloy*. Coatings 9 (2019), pp. 413.
- [12] J.X. Zou, T. Grosdidier, B. Bolle, K.M. Zhang, and C. Dong, *Texture and microstructure at the surface of an AISI D2 steel treated by high current pulsed electron beam*. Metall. Mater. Trans. A Phys. Metall. Mater. Sci. 38A (2007), pp. 2061–2071.
- [13] L.J. Chai, B.F. Chen, S.Y. Wang, Z. Zhang, and K.L. Murty, *Microstructural, textural and hardness evolution of commercially pure Zr surface-treated by high current pulsed electron beam*. Appl. Surf. Sci. 390 (2016), pp. 430–434.
- [14] J.X. Zou, K.M. Zhang, T. Grosdidier, and C. Dong, *Analysis of the evaporation and re-condensation processes induced by pulsed beam treatments*. Int. J. Heat Mass Transfer 64 (2013), pp. 1172–1182.
- [15] Y. Samih, G. Marcos, N. Stein, N. Allain, E. Fleury, C. Dong, and T. Grosdidier, *Microstructure modifications and associated hardness and corrosion improvements in the AISI 420 martensitic stainless steel treated by high current pulsed electron beam (HCPEB)*. Surf. Coat. Technol. 259 (2014), pp. 737–745.
- [16] L.Y. Zhang, C.T. Peng, J. Shi, and R.F. Lu, *Surface alloying of chromium/tungsten/stannum on pure nickel and theoretical analysis of strengthening mechanism*. Appl. Surf. Sci. 532 (2020), pp. 147477.
- [17] K.M. Zhang, J.X. Zou, T. Grosdidier, and C. Dong, *Formation and evolution of craters in carbon steels during low-energy high-current pulsed electron-beam treatment*. J. Vac. Sci. Technol. A 27 (2009), pp. 1217–1226.
- [18] K.M. Zhang, J.X. Zou, T. Grosdidier, N. Gey, S. Weber, D.Z. Yang, and C. Dong, *Mechanisms of structural evolutions associated with the high current pulsed electron beam treatment of a NiTi shape memory alloy*. J. Vac. Sci. Technol. A 25 (2007), pp. 28–36.
- [19] J.C. Pereira, J.C. Zambrano, E. Rayon, A. Yanez, and V. Amigo, *Mechanical and microstructural characterization of MCrAlY coatings produced by laser cladding: The influence of the Ni, Co and Al content*. Surf. Coat. Technol. 338 (2018), pp. 22–31.

- [20] J.C. Pereira, J.C. Zambrano, C.R.M. Afonso, and V. Amigo, *Microstructure and mechanical properties of NiCoCrAlYTa alloy processed by press and sintering route*. Mater. Charact. 101 (2015), pp. 159–165.
- [21] F. Ghadami, A.S.R. Aghdam, and S. Ghadami, *Abrasive wear behavior of nano-ceria modified NiCoCrAlY coatings deposited by the high-velocity oxy-fuel process*. Mater. Res. Express 6 (2019), pp. 1250d6.